In Situ Observation of Fringing-Field-Induced Phase Separation in a Liquid-Crystal–Monomer Mixture

Hongwen Ren and Shin-Tson Wu
College of Optics and Photonics, University of Central Florida, Orlando, Florida 32816, USA

Yi-Hsin Lin
Department of Photonics, Institute of Electro-Optical Engineering, National Chiao Tung University, Hsinchu 30010, Taiwan
(Received 31 July 2007; published 20 March 2008)

Fringing-field-induced phase separation dynamics in liquid-crystal–(LC-)monomer mixtures is investigated via a microscope. At a low LC concentration, the fringing field converts the randomly dispersed LC droplets to an ordered droplet array, while at a high LC concentration the fringing field converts the amorphous LC-monomer system to a composite film. Because the LC and monomer are immiscible, the converted morphologies are stable even after the voltage is removed. Using the fringing field-induced phase separation, it is possible to prepare different polymer-dispersed LC morphologies.

DOI: 10.1103/PhysRevLett.100.117801 PACS numbers: 61.30.−v, 42.70.Df, 77.84.Nh

Polymer-dispersed liquid-crystal (PDLC) is an attractive electro-optic medium which has been extensively studied for light switches [1,2], phase modulators [3–6], electronic lenses [7,8], and displays [9]. In a PDLC system, liquid crystal (LC) usually forms micron-sized droplets which are randomly dispersed in the polymer matrix. To form a PDLC, several factors, such as curing temperature, UV intensity, and the materials employed can influence the phase separation morphologies simultaneously in the phase separation process. Usually it is difficult to control precisely the phase separation morphology and predict where the LC droplets would appear in the polymer matrix. Once the phase separation is complete, the formed morphology cannot be changed because the polymer matrix has been solidified.

West's group [10,11] proposed a patterned electric field method to induce phase separation for preparing polymer walls. This method is attractive because the LC and monomers are already separated by the electric field before UV exposure. However, the LC molecules are in vertical alignment during the phase separation process and the ordinary refractive index of LC matches that of polymer, it is not easy to trace the phase separation process.

In this Letter, we use fringing electric fields to induce LC-monomer phase separation. Because the LC directors are reoriented by the fringing field, we can easily track the phase separation process. In our experiment, we found that phase separation morphologies are quite different before, during, and after the impacts of lateral electric fields. Various phase separation morphologies are obtained and results are compared based on the phase separation mechanisms. The fringing field method not only allows us to observe the *in situ* phase separation dynamics but also opens a new door to fabricate various electro-optic devices.

According to the Kelvin theory [12], when a dielectric object is placed in an inhomogeneous electric field, it bears a net force in the direction towards the higher field strength. The net force, called Kelvin polarization force, is proportional to the polarizability of the particle and the gradient of the electric field as [12]:

$$\vec{F} = \vec{P} \bullet \nabla \vec{E}, \tag{1}$$

where **P** is the induced dipole moment and ∇ is the del operator. Moreover, P is related to the electric field as

$$\vec{P} = \varepsilon_0(\varepsilon - 1)\vec{E}, \tag{2}$$

where ε_0 is the permittivity of free space and ε represents the dielectric constant of the particle. If this particle is surrounded by a medium whose dielectric constant is ε_m rather than air, then the net force on the particle has following form:

$$\vec{F} = \frac{\varepsilon_0}{2}\nabla[(\varepsilon - \varepsilon_m)E \bullet E] - \frac{1}{2}E \bullet E\nabla(\varepsilon - \varepsilon_m). \tag{3}$$

Equation (3) contains two terms, but the second term is either negligible or zero because ε and ε_m are both scalars. Therefore, the electric field gradient plays the key role to the force. The net force is zero when $\varepsilon = \varepsilon_m$. Moreover, the force changes sign depending on whether the particle's dielectric constant is larger or smaller than that of the surrounding medium.

Both LC and liquid monomer are dielectric materials but with different dielectric constants. If we treat the LC molecules as particles and monomer as the surrounding medium, it is possible to force them to be phase separated using an inhomogeneous electric field. To generate such an electric field, we used in-plane switching electrodes and the phase separation mechanism is shown in Fig. 1. The cell is composed of two glass substrates and an indium tin oxide (ITO) electrode. The ITO on bottom substrate surface is etched with interdigitated strips. A mixture of LC and liquid monomer is filled in the cell chamber in an

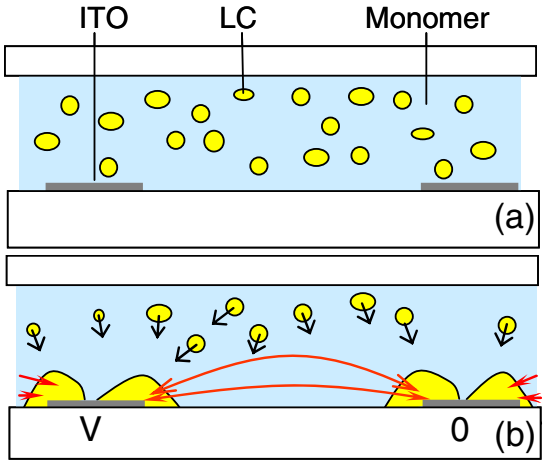

FIG. 1 (color online). Mechanism of fringing field enforced phase separation: (a) $V = 0$, (b) $V = V_1$.

isotropic state, as shown in Fig. 1(a). Initially, the LC in the solvent could keep the isotropic state or form droplets due to partial phase separation. When a voltage is applied to the ITO strips, the generated fringing field is inhomogeneous, as Fig. 1(b) shows. The field has a gradient and is strong and more uniform between the electrodes [13]. As a result, they experience a force-enforced movement by the electric field. Since the employed LC has a larger dielectric constant than the liquid monomer, i.e., $\varepsilon_{\mathrm{LC}} > \varepsilon_m$, according to Eq. (3) the LC molecules will bear a greater force from the electric field. Under such circumstances, the LC molecules or LC droplets are forced to move toward the high electric field regions while liquid monomers are pushed to the weak electric field regions, as depicted in Fig. 1(b). When the phase separation is complete, the formed morphology is stable due to the presence of the fringing fields. However, if the voltage is removed this balance is broken and the LC will be redistributed in the monomer solvent.

To study the phase separation dynamics, we first filled a cell with a mixture consisting of 30 wt % nematic LC (BL-003, $\varepsilon_{\parallel} \sim 22.4$) and 70 wt % monomer NOA65 (Norland Optical Adhesive, $\varepsilon_p \sim 5$ at 1 kHz). The ITO electrode on the bottom substrate surface was etched with interdigitated chevron patterns. The angle of the zigzag ITO strips is 150°. The width and gap of the electrode strips are 4 and 10 μm, respectively. The cell gap was measured to be $\sim$7 μm. The mixture was injected into the empty cell in an isotropic state.

The *in situ* phase separation morphology was observed by eye and recorded by a digital camera mounted on top of a microscope. The cell was placed on a microscope stage and sandwiched between two crossed polarizers. Initially, the field was dark because the mixture was in isotropic state. Because the LC and monomer are immiscible, to clearly observe the phase separation we intentionally decreased the cell temperature so that phase separation happened spontaneously. Locally, above the critical micelle concentration the structure formed has a minimal surface-to-volume ratio. This makes the emerged LC to form spherical droplets. Because of the LC birefringence, the droplets are observed clearly, as shown in Fig. 2(a). The LC droplets are randomly dispersed in the liquid monomer. When an electric field $E > 3\ V_{\mathrm{rms}}/\mu$m was applied to the electrodes, the emerged LC droplets were driven to the high electric field regions. Figure 2(b) shows the shifted LC droplets in the chevron shape at $E \sim 3\ V_{\mathrm{rms}}/\mu$m. Some droplets were elongated to form short segments already. The LC droplets are located around the edges of ITO strips, as Fig. 1 shows. As the electric field is increased to $E \sim 14\ V_{\mathrm{rms}}/\mu$m, the LC droplets are highly elongated and finally connected together to form zigzag lines along the ITO strips, as Fig. 2(c) shows. The transition time from Fig. 2(a) to Fig. 2(c) is $\sim$3 s. Because the LC concentration is only 30 wt % in the mixture, the observed LC strips are relatively narrow. The black lines in the middle of LC strips show the isotropic monomers forming a wall on the middle of ITO strips. The width of the monomer wall was measured to be $\sim$2 μm, which is less than the width (4 μm) of the ITO strips.

The phase separation morphology is very stable with the presence of the fringing fields. However, when the voltage is decreased, each LC strip will split into many short segments, as shown in Fig. 2(d). Within each half period of a chevron, the LC strip separates into three pieces. After removing the voltage, each piece quickly shrinks to a droplet, as Fig. 2(e) depicts. The dashed red (or gray) lines indicate the ITO strip position. It shows that the LC droplets are located at the ends and center of the adjacent zigzag joints. One can see that the LC droplets form an array. Even after several hours, the size and position of each droplet do

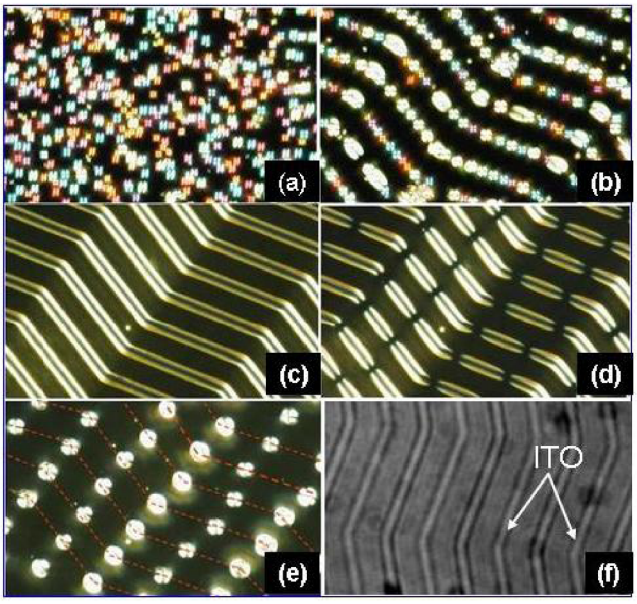

FIG. 2 (color online). Phase separation morphologies of 30 wt % BL-003 in 70 wt % NOA65 at room temperature: (a) $E = 0$, (b) $E = 3\ V_{\mathrm{rms}}/\mu$m, (c) $E = 14\ V_{\mathrm{rms}}/\mu$m, (d) $E = 3\ V_{\mathrm{rms}}/\mu$m, and (e) $E = 0$.

not change. Figure 2(f) shows the top view of the ITO pattern.

By comparing Fig. 2(a) with Fig. 2(e), we see that the phase separation before and after the impact of fringing electric fields is quite different. From Fig. 2(e), if this morphology is exposed under UV light, then the LC droplet array will be fixed permanently by a solid polymer matrix. Using this phase separation mechanism and different ITO patterns, one can prepare various LC droplet arrays. Such a method is much simpler than that using the monodisperse emulsion method [6].

To study the influence of LC concentration on the phase separation morphology, we prepared another cell with 75 wt % BL-003 in NOA65 solvent. The cell is the same as the first one except that its inner surfaces were coated with polyimide (PI) alignment layers. The PI layers were buffed in antiparallel directions; the rubbing axis is 15° with respect to the electrode strips. The reason that we use alignment layer is because of the high LC concentration in the mixture. Similar to the first cell, we observed the phase separation morphology using a polarizing optical microscope. When the LC cell is cooled to room temperature, LC droplets emerge very quickly from the monomer solvent, as shown in Fig. 3(a). The size distribution of the LC droplets is not uniform. When a voltage is applied to the ITO strips ($E \sim 3\ V_{\rm rms}/\mu$m), the dispersed LC droplets are flattened. As the voltage increases, the flattened LC domains begin to grow along the chevron ITO direction. During phase separation, we did not see the shifted LC droplets because LC is rich everywhere. When the flattened LC domains grow, they coalesce together with their neighbors and the surface covered by LC becomes larger, as shown in Fig. 3(b). When the electric field reaches $E \sim 12\ V_{\rm rms}/\mu$m, the chevron structures are clearly observed, as shown in Fig. 3(c). This chevron pattern is very similar to the structure of in-plane switching LC cell [14]. Similar to the walls observed in Fig. 2(c), the black grids imply that the monomer walls formed at the center of ITO strips. The width of the monomer wall was measured to be $\sim 1.5\ \mu$m. When the applied voltage is removed, the chevron structures disappear very quickly. Instead of forming LC droplets, the LC in the cell presents uniform color [green (or light gray)] with a few disclination lines, as shown in Fig. 3(d). By rotating the sample between the crossed polarizers, the darkest state is obtained if the rubbing direction of the cell is parallel or perpendicular to the fast axis of the polarizer. This result implies that the LC in the cell presents a homogeneous alignment.

Let us first explain the phase separation morphology of the cell with 75 wt % LC according to the phase separation mechanism. When the uniform mixture in the cell is cooled from a high temperature, phase separation takes place because the LC and monomer solvent are immiscible. When a high lateral electric field is applied to the ITO electrodes, LC and liquid monomers are forced to have anisotropic phase separation due to the net Kelvin force. Based on the experimental data observed from Figs. 3(c) and 3(d), we constructed a model shown in Fig. 4 to explain the final phase separation structure. Figure 4(a) shows the morphology of the cell after phase separation is complete. Here, only a small amount of monomer is in contact with the polyimide layer. The surface tension of LC ($\gamma_{\rm LC} \sim 15$ dyne/cm), monomer (NOA65 $\gamma_M \sim 36.4$ dyne/cm),

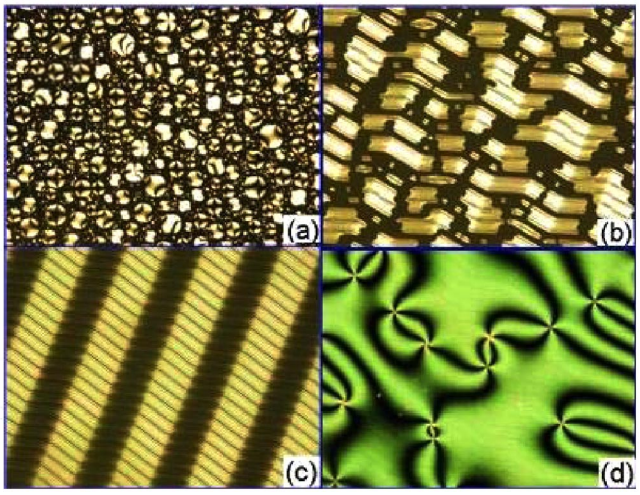

FIG. 3 (color online). Phase separation morphologies of 75 wt % BL-003 in 25 wt % NOA65 at room temperature: (a) $E = 0$, (b) $E = 3\ V_{\rm rms}/\mu$m, (c) $E = 12\ V_{\rm rms}/\mu$m, and (d) after removing the electric field.

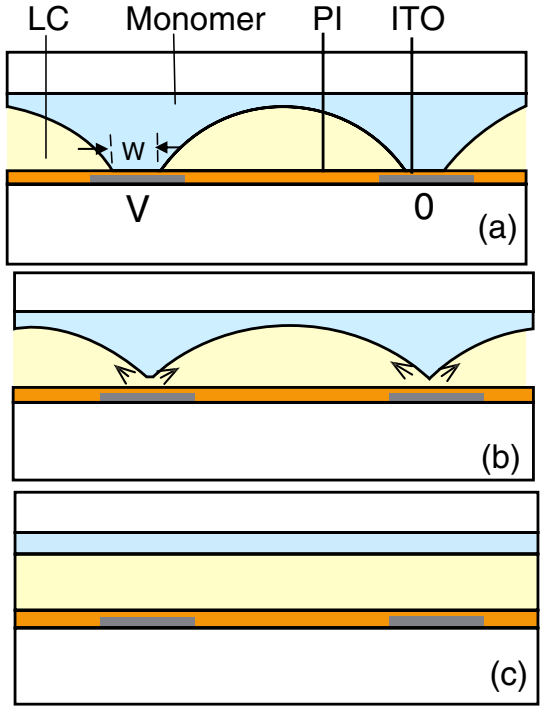

FIG. 4 (color online). Phase separation mechanisms of the second LC cell: (a) with a voltage, (b) during removing the voltage, and (c) final balanced state. **W** is the width of monomer walls.

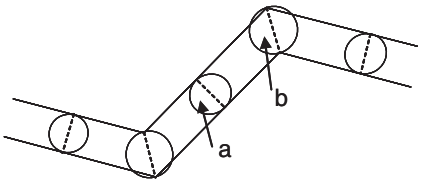

FIG. 5. LC droplets formed on the chevron ITO strip surface. The diameter of droplet a and droplet b is d_a and d_b, respectively.

and polyimide layer ($\gamma_P \sim 33$–42 dyne/cm) has the following order: $\gamma_{LC} < \gamma_M \sim \gamma_P$ [15]. Therefore, when the voltage is off the polyimide layer will adsorb LC rather than the monomer. As a result, the liquid monomer in the top layer has the tendency to shrink in order to minimize the surface energy, as depicted in Fig. 4(b). When the energy reaches a minimum, the morphology is stable, as shown in Fig. 4(c). The cell forms composite films. Because the alignment layer of the bottom substrate is gently rubbed, so the LC presents a homogeneous alignment. This is indeed observed in Fig. 3(d). If the monomer is cured by an UV light, then one would get a phase-separated composite film (PSCOF) [5]. In comparison with the previous method [5], our electric field-forced PSCOF can be easily fabricated with a wide range of LC layer thickness by adjusting either the LC cell gap, LC concentration, or both.

Similarly, the phase separation of the cell with 30 wt % LC can also be explained using the surface free energy. When the voltage is removed, the LC molecules in the curved side tend to expand and push the polymer wall up due to the interfacial tension. Therefore, the LCs tend to form a cylindrical strip on the ITO surface. However, this condition cannot sustain because the ITO surface tension is relatively weak. As a result, the LC strips tend to shrink. During shrinking process, the LC strips encounter resistance from the monomer, which causes the LC strips to break. Within each half period of a chevron, the LC strip breaks into three pieces. Usually the large area attracts more LC molecules and forms larger droplets. From Fig. 2(e), the LC droplets at the turning positions are relatively large. The middle piece contains fewer LC molecules so that the droplets located in the center are smaller. To explain this phenomenon, we suppose that LC is confined only on the ITO surface by the liquid monomer, as shown in Fig. 5. Because of the chevron ITO pattern, the diameter (d_a) of droplet a is near to the width of ITO strip. On the other hand, the diameter (d_b) of droplet b is equal to the length of the conjoined segment. Therefore, d_b is slightly larger than d_a. In our LC cell, forming the LC droplet and evicting the monomer wall take place at the same time. After removing the voltage, the formed LC droplet array in monomer solvent remains very stable.

In comparison with previous methods, our fringing-field-induced phase separation can produce different morphologies depending on the LC concentration and the electric field. For instance, at a low LC concentration the mixture can be forced to form a grating pattern by the lateral electric fields. Removing the voltage would lead to LC droplet array. On the other hand, at high LC concentration the electric field can induce polymer walls, where LC is enclosed inside the walls. If the voltage is removed, then after the second phase redistribution the mixture would exhibit PSCOF morphology.

In summary, the phase separation dynamics induced by an external fringing field is investigated. Our results show that before, during, and after the impact of a fringing field, the phase separation morphology can be converted from one state to another stable state. At a low LC concentration, the initially randomly dispersed LC droplets are converted to a droplet array, while at high LC concentration the randomly dispersed LC droplets are merged to form a double-layer composite film. By considering various important factors, such as substrate surface tension, LC concentration, ITO pattern, and electric field (including vertical and lateral) directions, various phase separation morphologies can be obtained.

The authors are indebted to Chang-Ching Tsai and Zhibing Ge for valuable discussions and Benjamin Wu for proofreading the manuscript.

[1] J. W. Doane, N. A. Vaz, B. G. Wu, and S. Zumer, Appl. Phys. Lett. **48**, 269 (1986).
[2] P. S. Drzaic, J. Appl. Phys. **60**, 2142 (1986).
[3] R. L. Sutherland, L. V. Natarajan, V. P. Tondiglia, and T. J. Bunning, Chem. Mater. **5**, 1533 (1993).
[4] H. Ren, Y. H. Lin, Y. H. Fan, and S. T. Wu, Appl. Phys. Lett. **86**, 141110 (2005).
[5] V. Vorflusev and S. Kumar, Science **283**, 1903 (1999).
[6] A. Fernandez-Nieves, D. R. Link, D. Rudhardt, and D. A. Weitz, Phys. Rev. Lett. **92**, 105503 (2004).
[7] H. Ren and S. T. Wu, Appl. Phys. Lett. **81**, 3537 (2002).
[8] H. Ren, Y. H. Fan, Y. H. Lin, and S. T. Wu, Opt. Commun. **247**, 101 (2005).
[9] R. Penterman, S. I. Klink, H. de Koning, G. Nisato, and D. J. Broer, Nature (London) **417**, 55 (2002).
[10] Y. Kim, J. Francl, B. Taheri, and J. L. West, Appl. Phys. Lett. **72**, 2253 (1998).
[11] N. Gheorghiu, J. L. West, A. V. Glushchenko, and M. Mitrokin, Appl. Phys. Lett. **88**, 263511 (2006).
[12] J. D. Jackson, *Classical Electrodynamics* (Wiley, New York, 1975), 2nd ed.
[13] Z. Ge, X. Zhu, T. X. Wu, and S. T. Wu, J. Soc. Inf. Disp. **14**, 1031 (2006).
[14] H. Ren, S. T. Wu, and Y. H. Lin, Appl. Phys. Lett. **90**, 191105 (2007).
[15] J. Cognard, Mol. Cryst. Liq. Cryst., Suppl. Ser. **1**, 1 (1982).